https://doi.org/10.31689/rmm.2024.31.2.155

ORIGINAL PAPERS

A Method Utilizing an Image Visibility Graph to Portray the Arrangement of Genomic Data Sequencing, Gene Frequencies for The Peptidoglycan-Associated Lipoprotein (Pal) Gene in Brucella Spp., and Prevalence of Brucellosis in Nineveh

Ali Adel DAWOOD

Abstract

Brucellosis is a disease triggered by various Gram-negative bacteria (Brucella spp.), impacting animals through miscarriages and causing fever in humans. The verified reality that peptidoglycan-associated lipoprotein (Pal) proteins exist in multiple bacteria and display remarkable vaccine potential shifts the spotlight to this protein and its importance within bacterial systems. Furthermore, gaining insight into the implications of mutations in this protein becomes of utmost importance. Biological informatics software was utilized to carry out a comparative study of the Pal gene across different species of Brucella bacteria. Computational methods were employed to represent sequences using both CGR and FCGR techniques. The Pal protein's secondary and tertiary structures were built, and comparisons were drawn regarding mutations present among various Brucella species. An assessment of instances of infection was conducted, and statistical analyses were executed concerning brucellosis in the Nineveh region. While no significant differences were observed in the Pal gene among Brucella species, noticeable variations became evident when employing CGR and FCGR methodologies. FCGR proves to be more precise for visualization compared to CGR. Particularly, B. endophytica exhibited the most notable changes in the Pal protein when compared to the standard type within the species. The frequency of brucellosis infections increases in correlation with rising population numbers. The initial CGR images might not exhibit noticeable differences, but utilizing the FCGR method makes it easier to distinguish these variations. This affirms that FCGR is more effective for assessing the degree of dissimilarities. The presence of brucellosis poses a concern, especially in regions characterized by dense populations. It is important to emphasize public education regarding the adoption of suitable health precautions to thwart the disease, coupled with the importance of vaccination..

Keywords: Brucella, Pal, gene expression, FCGR, 3D structure.

[1]Microbiology, College of Medicine, University of Mosul, Mosul, Iraq

*Corresponding author:
Ali Adel DAWOOD, Microbiology, College of Medicine, University of Mosul, Mosul, Iraq
E-mail: aad@uomosul.edu.iq

INTRODUCTION

Brucellosis is a disease caused by a type of Gr-ve bacteria (Brucella spp). that affects animals causing miscarriage and humans causing fever (Malta fever, undulant fever, or Mediterranean fever)[1]. This disease is characterized by intermittent and irregular fever, headache, general weakness and fatigue, profuse sweating with chills, joint pains, back pain, weight loss, and enlargement of the liver and spleen. The infected person may suffer from the disease for a long period, which can extend to years if not treated promptly[2].

Domesticated animals (such as camels, sheep, and cattle) are the main source of the disease. Intensive livestock farming accelerates the spread of the disease among animals. Uterine discharges, placenta, raw meat, liver, and milk contain disease-causing microbes[3]. The disease can be transmitted through skin contact, especially among those handling infected animal meat, like butchers. It can also be transmitted through mucous membranes, like the conjunctiva and the respiratory system, as well as by consuming unpasteurized milk or its products and raw liver from infected animals[4,5].

A combination of two or more treatments is usually employed, especially for chronic cases, and particularly if complications arise. Doxycycline at a dose of 2-4 mg/kg/day for four to six weeks is used along with trimethoprim, both for the same duration. For severe complications such as bone inflammation, meningitis, and pericarditis, streptomycin or gentamicin is administered. Rifampicin is used to reduce the risk of relapse. Doxycycline is not given to children under the age of eight[6,7].

The peptidoglycan-associated lipoprotein (Pal) is an evolutionarily conserved lipoprotein situated within the outer membrane of Gram-negative bacteria. In the context of the Tol-Pal family, Pal assumes a critical role in maintaining the structural integrity of the cell wall. However, its function extends beyond this foundational role to include an inflammatory trigger. For example, in *B. abortus* infections, Pal is one of the lipoproteins responsible for inducing the production of cytokines that promote inflammation in cases of brucellosis[8,9]. The Tol-Pal proteins collectively form a complex that spans both the inner and outer membranes of the bacterial cell. This intricate arrangement is indispensable for upholding the robustness of the cell wall. Furthermore, this complex mechanism can be harnessed to facilitate the entry of large molecules, such as bacteriocins and bacteriophages[10,11].

The primary goal of this study was to apply the Chaos for game representation method to facilitate a comparative analysis of the DNA sequences of the Pal gene within specific strains of Brucella. Additionally, the research encompassed the construction of the three-dimensional structure of the Pal protein, followed by a comparison with corresponding structures found in mutant strains. Furthermore, the investigation incorporated a statistical analysis to assess the prevalence of brucellosis within the province of Nineveh.

MATERIALS AND METHODS

MSA and Phylogenetic tree:

MAFFT version 7 was employed to align a set of eight Pal protein sequences and five Pal gene sequences from diverse Brucella species. Subsequently, a phylogenetic tree was constructed based on these aligned sequences.

The Chaos Game Representation (CGR) is a visualization technique used to represent DNA sequences in a fractal-like manner[12]. It's a method to graphically display the distribution of nucleotides within a DNA sequence. The Pal gene from five Brucella species was chosen from the NCBI database for this study. These species include: *B. melitensis* (NC_003317.1), *B. canis* (NC_010103.1), *B. abortus* (NC_007618.1), *B. anthropic* (NZ_CP064063.1), and *B. intermedia* (NZ_UGSH01000003.1). *B. melitensis* served as the wild type reference for comparison with the other species.

The approach to assigning sequential numbers to nucleotides within a given DNA sequence. The methodology involves the establishment of a counting system that aligns each nucleotide with a unique numerical value corresponding to its position within the sequence. This process is crucial for data organization and subsequent analysis, facilitating the identification of specific nucleotides within a broader genomic context. The 2D grid or plot was utilized, with the origin conventionally positioned at the center of the grid. This grid was divided into four quadrants to symbolize the four DNA nucleotides (A, T, G, C). Each nucleotide was placed on the grid based on its location in the DNA sequence, aligned along the x- and y-axes (x,y). Here is how the first 6 nucleotides (ATGCGC) were positioned:

A: The A quadrant is the top-left quadrant. The midpoint between the current position (0, 0) and the position of A (0, 1) is ((0 + 0) / 2, (0 + 1) / 2) = (0, 0.5).

T: The T quadrant is the top-right quadrant. The midpoint between the current position (0, 0.5) and the position of T (1, 1) is ((0 + 1) / 2, (0.5 + 1) / 2) = (0.5, 0.75).
G: The G quadrant is the bottom-left quadrant. The midpoint between the current position (0.5, 0.75) and the position of G (0, 0) is ((0.5 + 0) / 2, (0.75 + 0) / 2) = (0.25, 0.375).
C: The C quadrant is the bottom-right quadrant. The midpoint between the current position (0.25, 0.375) and the position of C (1, 0) is ((0.25 + 1) / 2, (0.375 + 0) / 2) = (0.625, 0.1875).
G: The G quadrant is the top-left quadrant. The midpoint between the current position (0.625, 0.1875) and the position of G (0, 1) is ((0.625 + 0) / 2, (0.1875 + 1) / 2) = (0.3125, 0.59375).
C: The C quadrant is the top-right quadrant. The midpoint between the current position (0.3125, 0.59375) and the position of C (1, 1) is ((0.3125 + 1) / 2, (0.59375 + 1) / 2) = 0.65625.
Subsequently, after each nucleotide assignment, the counter is increased by 1, thus preparing it for the subsequent iteration. Ultimately, the mapping of nucleotides to their corresponding numbers is established through the cumulative impact of this iterative procedure. This cumulative process is captured by the accumulation equations presented as follows:
new_x = current_x + (∑ (target_x - current_x) / 2^n)
new_y = current_y + (∑ (target_y - current_y) / 2^n).
The process of Frequency Chaos Game Representation (FCGR) entails computing how often a specific pattern occurs within a sequence and then depicting this occurrence frequency using a chaos game plot[13]. This is accomplished by associating varying color intensity or grayscale shades with each point on the plot, which is determined by the frequency of the motif element at that position in the sequence. The resulting FCGR plot provides a visual insight into the pattern's distribution in the sequence, where increased motif frequency is depicted through darker areas. The FCGR method was executed following the described approach:
Frequency(M) = (Number of times motif M occurs in sequence S) / (n - k + 1)
S: Represents the sequence you are analyzing.
n: Represents the length of the sequence. If S is a DNA sequence, n would be the number of nucleotides in the sequence.
M: Represents the motif that it is interested in identifying within the sequence.
k: Represents the length of the motif.

Construction of 2D and 3D structures of Pal protein: The 2D structure of Pal proteins was generated using the PROTEUS2 and PRED-TMR2 tools. The prediction of the tertiary structure for the Pal protein in five Brucella species, including *B. melitensis* (WP_005972694.1), *B. abortus* (WP_002964783.1), *B. gallinifaecis* (WP_140905268.1), *B. thiophenivorans* (WP_094505464.1), and *B. endophytica* (WP_188824549.1), was conducted using the 3Dpro tertiary structure prediction tool from the SCRATCH Protein Predictor. The protein sequences were graphically represented, and mutations were detected and then manipulated utilizing the PyMol software tool.

Information regarding brucellosis cases, including their numerical counts, was collected from the Nineveh Health Department. A comprehensive statistical analysis was carried out on this data, followed by the creation of graphical plots to visualize the trends. Using SPSS version 20, significant values were identified and extracted from the analyzed data.

RESULTS

B. melitensis was deemed a reference point for all bacterial species in various examinations. Analysis of multiple sequence alignments revealed the existence of 28 significant mutations within the *Pla* gene classifications. These mutations do not exert a direct influence on the final protein configuration. In relation to the phylogenetic tree investigation, predicated on the scrutiny of multiple sequence alignments, it becomes apparent that *B. melitensis* and *B. abortus* are the nearest species. The remaining species align themselves based on their genetic proximity, as demonstrated in Figure 1. Upon analyzing the DNA sequence plots of the Pal gene among different Brucella species, no substantial alteration was noted among the five species. The graphical representation of the DNA sequence exhibits a nearly identical curve, with a similarity level surpassing 96%, as illustrated in Figure 2.

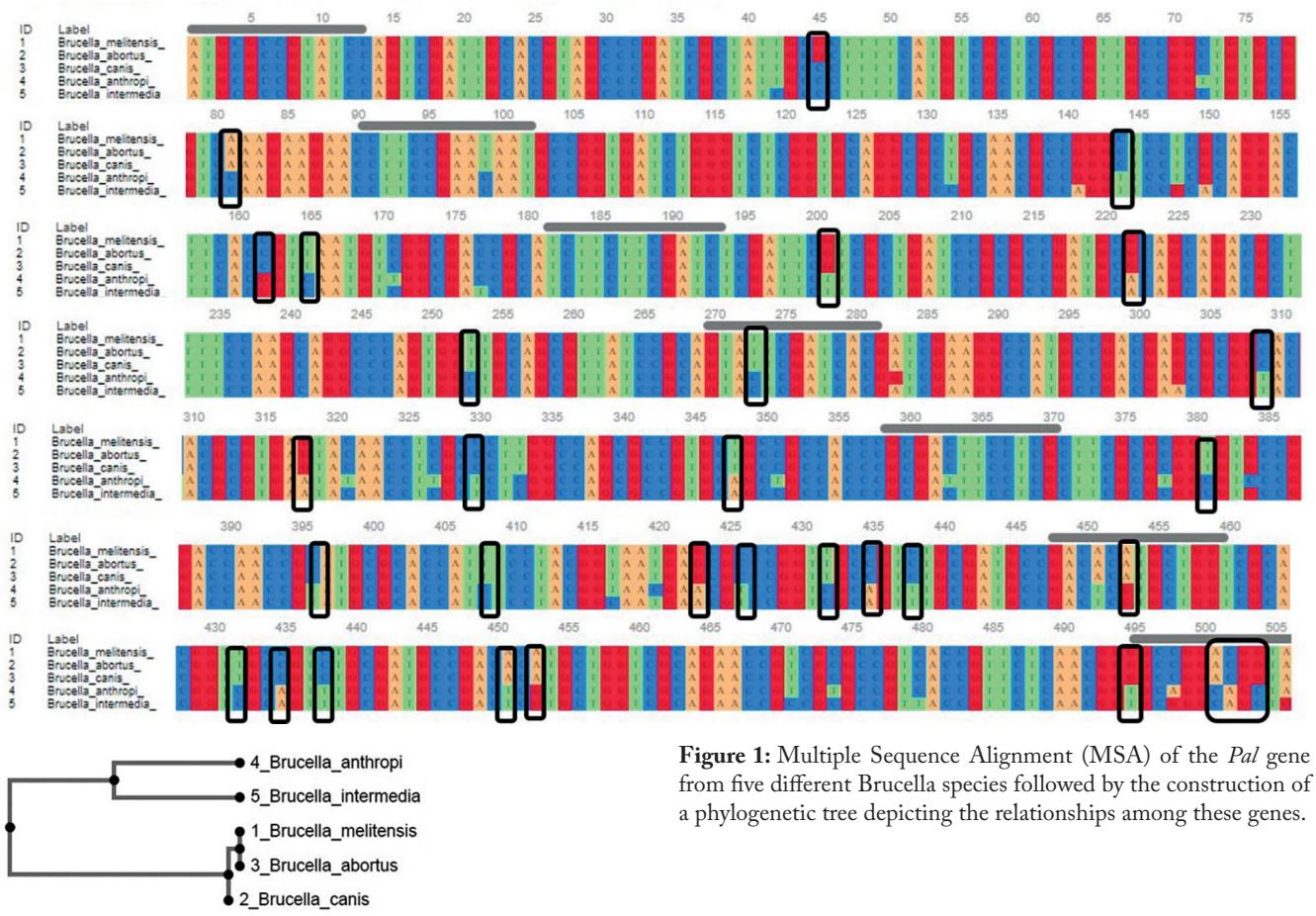

Figure 1: Multiple Sequence Alignment (MSA) of the *Pal* gene from five different Brucella species followed by the construction of a phylogenetic tree depicting the relationships among these genes.

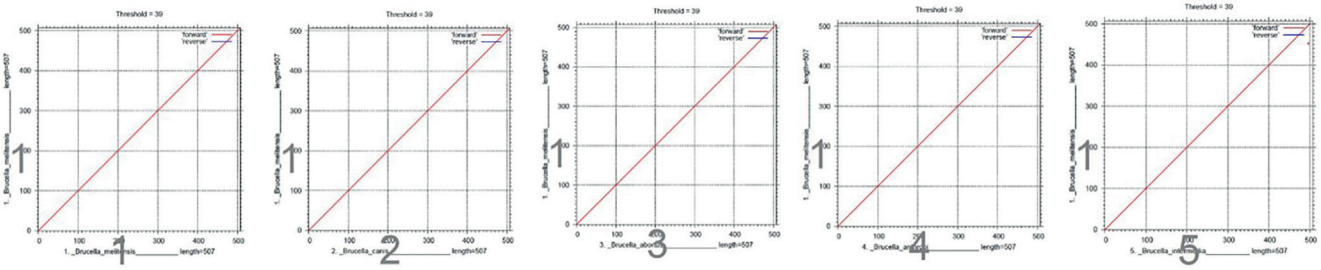

Figure 2: Graphical representations were created to compare the *Pal* gene of various Brucella species: Plot 1 displays a comparison between the *Pal* gene of *B. melitensis*. Plot 2 contrasts the *Pal* gene of *B. melitensis* and *B. canis*. Plot 3 illustrates a comparison between the *Pal* gene of *B. melitensis* and *B. abortus*. Plot 4 showcases a comparison between the *Pal* gene of *B. melitensis* and *B. antropi*. Plot 5 demonstrates a comparison between the *Pal* gene of *B. melitensis* and *B. intermedia*.

Concerning the multiple sequence alignments of the Pal protein, 8 distinct fundamental mutations are evident among bacterial species, except for *B. endophytica*. Notably, there exists a substantial divergence within the sequence spanning positions 45 to 48 residues. The protein-based phylogenetic analysis within the species bears a resemblance, to some extent, to the gene-derived phylogenetic tree, as depicted in Figure 3.

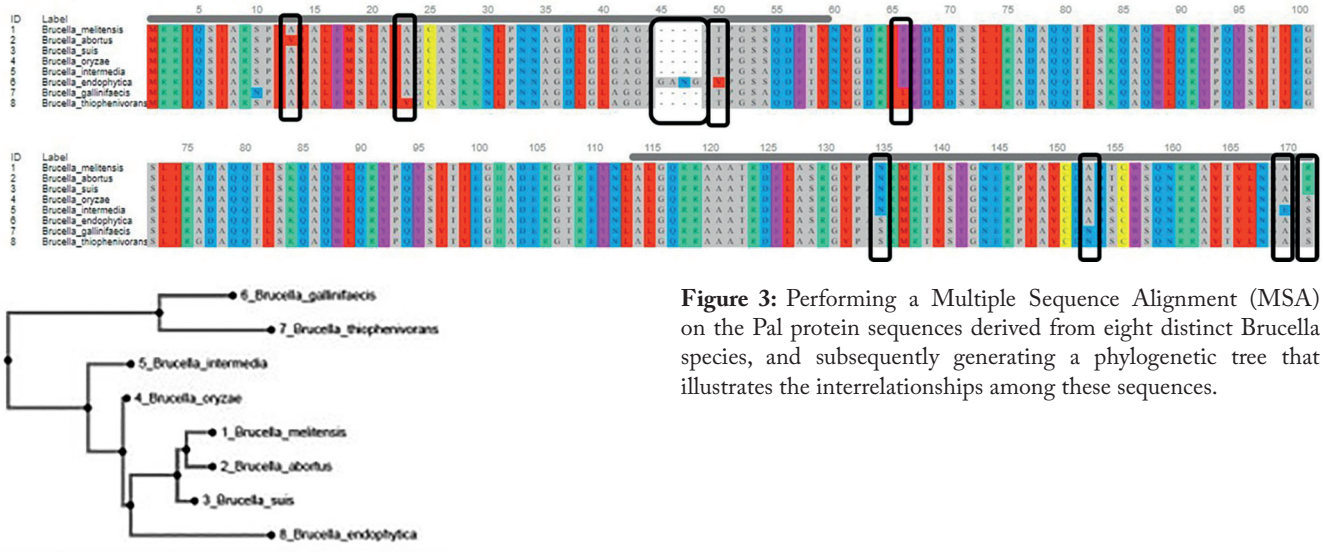

Figure 3: Performing a Multiple Sequence Alignment (MSA) on the Pal protein sequences derived from eight distinct Brucella species, and subsequently generating a phylogenetic tree that illustrates the interrelationships among these sequences.

After conducting a comprehensive DNA sequence imaging of the *Pal* gene across various Brucella species, with *B. melitensis* as a baseline model presented in Figure 4. a noteworthy level of resemblance was observed among the species, reaching an approximate value of 70%. *B. melitensis* displayed an 80% similarity rate with both *B. canis* and *B. abortus*. Conversely, the degrees of similarity with *B. anthropic* and *B. intermedia* differed, showing an affinity of around 60%. This visualization provides a comprehensive overview of the genetic disparities within the *Pal* gene among different Brucella species, enabling a quick and intuitive understanding of the extent of genetic variation.

To provide a clearer insight into the levels of similarity among the strains, frequency imaging was employed. This process entailed incorporating four nucleotides into the representation of the DNA sequence. By analyzing the results of frequency imaging for the DNA sequence among the five species depicted in Figure 5, utilizing the same previously mentioned methodology, it becomes evident that the species *B. melitensis, B. canis*, and *B. abortus* exhibit a similarity of approximately 85%. In contrast, the species *B. anthropic* and *B. intermedia* diverge from the rest, showcasing a dissimilarity of about 65%. By utilizing this visualization, the genetic disparities within the *Pal* gene across different Brucella species are effectively showcased based on the gradual accumulation of base pairs, offering insights into the degree of genetic variation among these species.

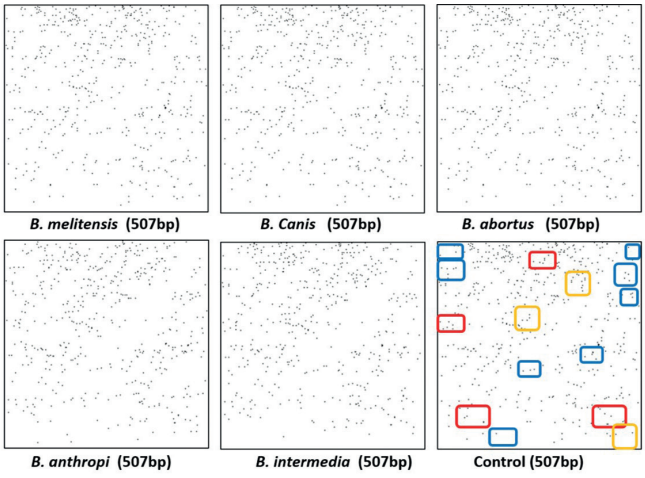

Figure 4: CGR of the Pal gene across various Brucella species reveals distinct variations. In this representation, specific differences between nucleotides are denoted using different colors and circle sizes. The blue square highlights variations between 2 nucleotides, showcasing moderate disparities. The red square indicates differences involving 4 nucleotides, representing more substantial distinctions. Notably, the yellow square signifies variations exceeding 5 nucleotides, indicating significant dissimilarity.

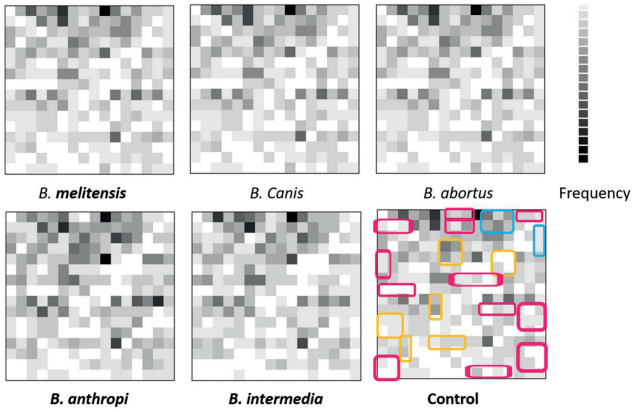

Figure 5: FCGR of the Pal gene in various Brucella species, organized by the gradual accumulation of 4 base pairs along the DNA sequences. This representation employs different colored squares to indicate variations between species: The pink square denotes differences in one set of base pairs between species, highlighting minor distinctions. The blue square signifies differences in 2 sets of base pairs between species, representing more significant differences. The yellow square indicates variations of more than 2 sets of base pairs between species, pointing to substantial dissimilarities.

Through the application of two-dimensional structural prediction to the Pal protein across 8 different Brucella species, a notable finding emerges: these diverse species exhibit a substantial 90% similarity. A noteworthy differentiation becomes evident within the amino acids positioned at residues 165- 168. This similarity is observed in distinct species, included *B. melitensis, B. abortus, B. gallinifaecis*, and *B. thiophenivorans*. However, *B. endophytica* deviates from this established pattern, demonstrating a similarity rate of 70% when compared to the other species, Figure 6. This comparison sheds light on the differences within the Pal protein across these species.

A 3D configuration was crafted for the Pal protein within the examined species. Figure 7 depicts the 3D structures representing four specific species: *B. melitensis, B. suis, B. oryzae*, and *B. intermedia*. The distinctive residues among these four Brucella species, setting them apart from the others, have been recognized.

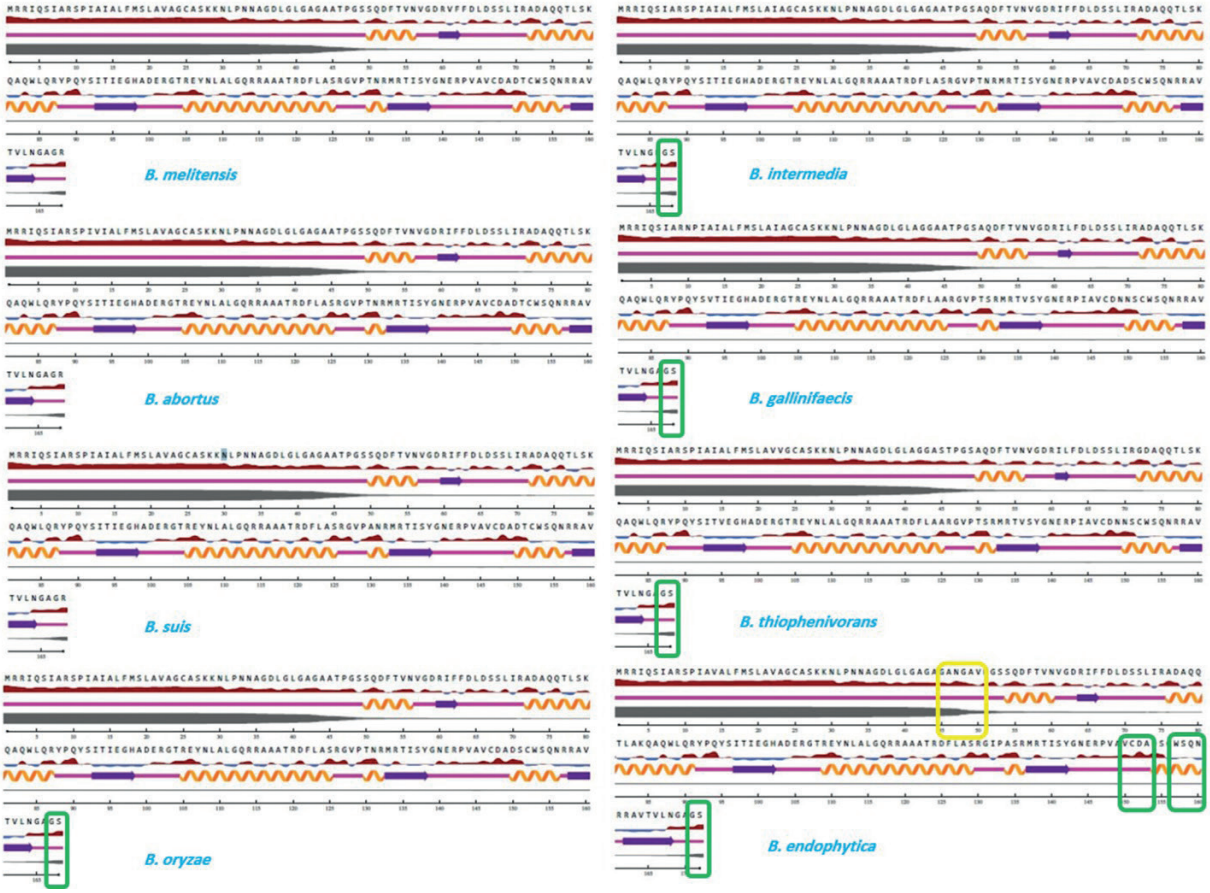

Figure 6: Analyzing the Pal protein across 8 Brucella species via two-dimensional structure prediction reveals distinct variations. The presence of a blue rectangle indicates discrepancies between species at residues 165-168. Notably, B. endophytica stands out with additional alterations in amino acids at residues: 50-54, 150-153, and 157-160.

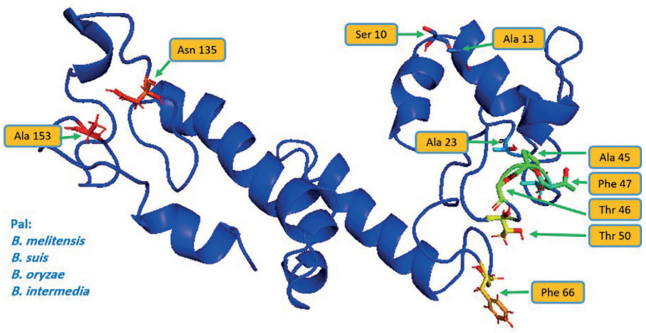

Figure 7: Anticipated 3D configuration of the Pal protein in *B. melitensis, B. suis, B. oryzae*, and *B. intermedia*, revealing the presence of the ten original residues: Ser13, Ala13, Ala23, Ala45, Thr46, Phe47, Thr50, Phe66, Asn135, and Ala153.

These residues encompass Ser13, Ala13, Ala23, Ala45, Thr46, Phe47, Thr50, Phe66, Asn135, and Ala153.

Figure 8 exhibits the remaining Brucella species carrying modifications in the Pal protein. In *B. abortus*, a sole mutation A13V is evident. Meanwhile, *B. gallinifaecis* displays 4 mutations: S10N, F66L, N135S, and A153N. Similarly, *B. thiophenivorans* showcases 4 mutations: A23V, F66L, N135S, and A153N. Noteworthy is the case of *B. endophytica*, manifesting 5 mutations: A45G, T46A, P47N, T50V, and N135S.

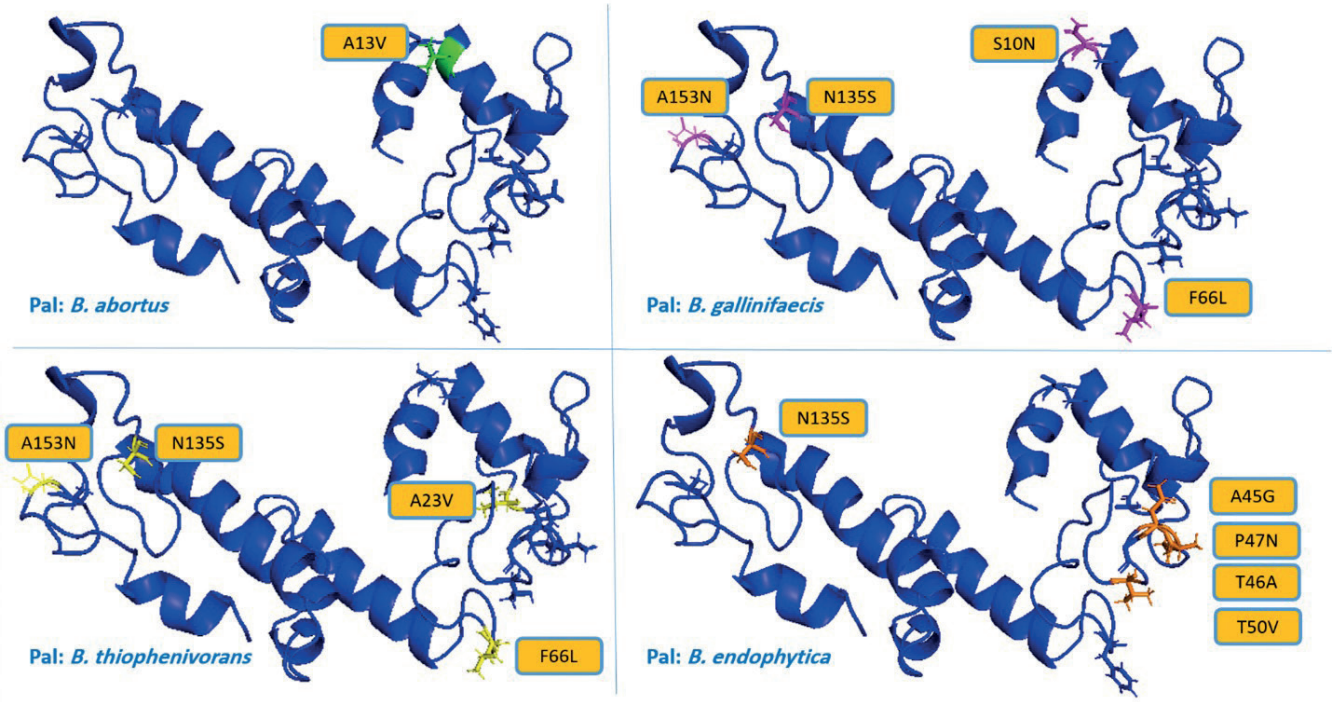

Figure 8: Genetic mutaions observed in the Pal protein within *B. abortus, B. gallinifaecis, B. thiophenivorans*, and *B. endophytica.*

Brucellosis is categorized as an indigenous ailment prevalent in Iraq overall and notably concentrated in the Nineveh. This concentration is attributed to its transmission among cattle and sheep, as well as the insufficiency of vaccination endeavors by the veterinary sector. The frequency of occurrence varies relative to the population size. An assessment of infections was executed spanning the years 2018-2022. While fluctuations in infection rates are apparent, it was noted that the peak instances transpired in 2022, without any noteworthy divergence in infection counts between males and females. Infections tend to be most commonly documented within the age bracket of 15-45 years, which aligns with a universally acknowledged trend. The instances are least frequent among those under 4 years old. A statistically significant relationship exists among infection numbers, age groups, and genders with a significance level of $p < 0.01$, illustrated in Table 1 and Figure 9.

Table 1: Brucellosis cases by age group and gender 2018 - 2022, Nineveh- Iraq.

Years	< 1y		1-4y		5-14y		15-45y		> 45y		TOTAL		Grand Total
	M	F	M	F	M	F	M	F	M	F	M	F	
2018	0	1	10	16	106	105	292	379	77	98	485	599	1084
2019	0	0	7	4	74	62	335	393	90	107	506	566	1072
2020	0	0	0	9	52	66	241	243	67	64	360	382	742
2021	0	0	4	2	64	51	209	281	72	92	349	426	775
2022	0	0	1	0	54	58	300	408	145	188	500	654	1154
TOTAL	0	1	22	31	350	342	1377	1704	451	549	2200	2627	4827

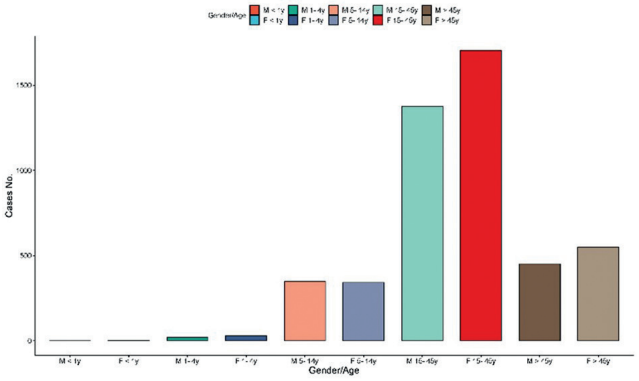

Figure 9: Brucellosis cases by age group and gender 2018 - 2022, Nineveh- Iraq.

In terms of the distribution of infections across different regions within Nineveh, it was observed that the highest concentration of infections was situated on the eastern side of Mosul, attributed to the dense population in that area. Areas characterized by intensified cattle and sheep farming activities, like Hadhar, Ba'aj, Hamdaneya, and Makhmoor, registered the most infections during the five-year scope of this study. However, when considering the years of statistical analysis, no substantial correlation emerges between infection numbers and the impacted areas, with a p-value surpassing 0.05. This is presented in Table 2 and Figure 10.

Table 2: Brucellosis cases by districts 2018-2022, Nineveh-Iraq.

Years	Mosul western side	Mosul eastern side	Talafar	Sinjar	Ba'aj	Talkeif	Sheekhan	Hamdaneya	Qayara	Hadhar	Makhmoor	Other sub-district	Total
2018	202	468	20	57	30	13	53	127	3	80	31	0	1084
2019	130	354	1	7	34	58	32	246	11	99	98	2	1072
2020	39	151	7	3	49	33	88	89	3	143	135	2	742
2021	27	126	0	1	111	20	49	55	167	85	129	5	775
2022	35	154	3	2	400	6	34	81	38	255	146	0	1154
Total	433	1253	31	70	624	130	256	598	222	662	539	9	4827

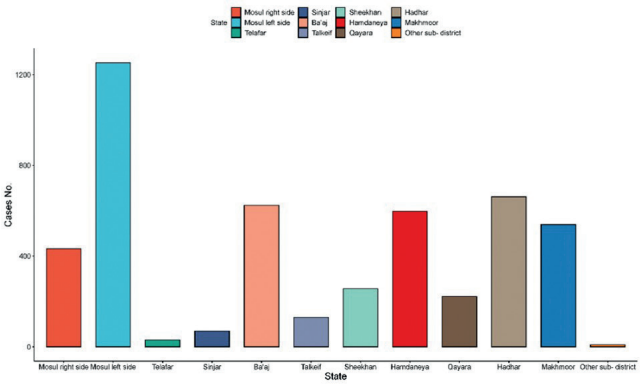

Figure 10: Brucellosis cases by districts 2018-2022, Nineveh-Iraq.

DISCUSSION

The Pal protein derived from Brucella bacteria possesses the ability to stimulate dendritic cells, prompting the release of the cytokine TNF-α. Additionally, Pal can activate macrophages, driving them to produce an array of cytokines, thereby playing a crucial role in the bacteria's virulence. Recent reports highlight the Brucella Pal protein as a novel Pathogen-Associated Molecular Pattern, capable of activating dendritic cells within living organisms. This activation triggers a Th1 immune response and positions it as a potential self-adjuvanting vaccine candidate against both systemic and orally acquired Brucellosis[14,15].

Study's findings have pointed out disparities in the roles of Brucella Pal proteins in stimulating macrophages to secrete cytokines. The precise reasons behind these functional variations necessitate additional experimental validation. Brucella exhibit the capability to survive within professional phagocytes, and internalized Brucella particles are transported alongside macrophages to different host sites[16, 17].

A study demonstrated that deleting the pal gene led to a reduction in Brucella proliferation within macrophages. In the macrophage environment, Brucella employs diverse strategies to counteract acidic and oxidative stress, as well as antimicrobial peptides, to enhance its survival and subsequent multiplication[18,19].

Further investigation delved into assessing the virulence of the pal mutant in BALB/c mice. The results indicated that mice challenged with 16MΔpal displayed notably enlarged spleens, surpassing even those challenged with the wild-type strain 16 M. However, the bacterial load in the spleen of 16MΔpal was lower than that in 16 M. Reports have indicated that Brucella's Pal protein can impede the secretion of IL-1β and IL-6 by macrophages. Conversely, in the absence of the Pal gene, the expression of IL-1β and IL-6 is elevated, which corresponds to a decrease in the virulence of the mutant strain[20, 21].

The Chaos Game Representation (CGR) picture and the FCGR expression matrix derived from DNA sequences offer an innovative technique for scientists to manipulate genetic information. Historically, researchers have employed CGR and fractal analyses of genetic sequences to determine the fundamental bases for categorization and grouping[12,13]. Our approach introduces a computational method for the automatic recognition of Pal gene strains within the Brucella species. Furthermore, this approach facilitates the identification of mutant strains within taxonomy by utilizing the variant coefficient linked to the DNA sequence label. As a result, our study of identifying the mutant strain not only validates our inspiration but also contributes to discerning dissimilarities among strains.

The devised methodology showcases an effective means of attributing sequential numbers to nucleotides within DNA sequences. The approach offers a straightforward and clear method for organizing genetic data in a manner conducive to subsequent analytical investigations. The application of numerical assignment is particularly valuable in studies involving sequence comparisons, motif identification, and other bioinformatics analyses.

The utilization of conventional techniques for detecting distinctions within DNA sequences, proteins, or what is commonly referred to as sequence alignment, remains the most precise method for identifying variations among strains. Nevertheless, variations in the manner by which these distinctions are identified can be observed when employing different bioinformatics programs. In this research, traditional approaches were employed to identify sequence alignment for the Pal gene and protein, using available and selected strains from the NCBI database.

Subtle variances were discerned among the various *Pal* gene types within the Brucella species. Utilizing the CGR method to discern differences among these species clarified that distinct differences exist among the five Brucella species when compared to the outcomes from the MAAFT program. By generating visual representations, significant differences were identified among the species to varying degrees, employing

both mathematical and computational methodologies. In regard to the utilization of the frequency-based FCGR, a selection of four nucleotides was made and organized into geometric patterns. These patterns were distributed at random around clusters of nitrogen bases within each geometric shape, based on the position of each nucleotide in the sequence. Furthermore, when juxtaposed with the traditional method of measuring sequence alignment, differences were observed in the *Pal* gene for Brucella species, and the values of variables were established to ascertain whether the alteration encompassed two sets between each pair of species, or three or more sets, with the ultimate goal of estimating differentiation among the five species[22,23].

While the initial CGR images may not reveal significant apparent differences, the application of the FCGR method enables these variations to be easily discerned, thus confirming that FCGR is better suited for gauging the extent of differences. Finally, through an examination of Pal protein sequences across the eight Brucella species, this study uncovered exceedingly slight differences in the formation of secondary protein structures. Conversely, after integrating specific mutations for Pal protein species into the three-dimensional framework, it became evident that four species shared a similar structural arrangement in their tertiary structures. In contrast, the remaining species exhibited dissimilarities among themselves based on the positions of these mutations, ultimately leading to alterations in the protein's shape. Notably, *B. endophytica* displayed significant dissimilarity from the other species due to possessing the top five mutations characteristic of the identified wild type[24].

Brucellosis is classified as one of the endemic ailments in Nineveh. The frequency of infections varies annually, contingent upon economic and health conditions. Moreover, infection rates between males and females exhibit minimal divergence. Additionally, the majority of documented infections occur within the age range of 15- 44 years. When comparing infection figures between the city and its surrounding areas, including districts and regions, it becomes evident that infection prevalence corresponds directly to the population size.

CONCLUSION

The process of assigning sequential numbers of nucleotides in a DNA sequence proves to be a fundamental tool for genomic research. The established approach facilitates systematic organization and analysis of genetic information, enhancing the comprehension and utilization of DNA sequence data in various scientific contexts. The confirmed fact that Pal proteins present in numerous microorganisms exhibit remarkable potential as vaccines directs focus towards this protein and its significance within bacteria. Additionally, understanding the consequences of mutations in this protein becomes pivotal. In a nation such as Iraq, the existence of brucellosis represents a threat, particularly in areas with high population density. It holds significance to educate the public about adopting appropriate health measures to prevent the illness, alongside receiving vaccination.

Acknowledgements No applicable.

Ethical Approval

The Ethics Committees at the College of Medicine, University of Mosul, ensured that informed consent was acquired from all the individuals participating in the study.

Competing interests

There are no financial conflicts of interest.

Authors' contributions

A single researcher presented this study and was responsible for conducting all aspects of the research.

Funding

This study was carried out at the researcher's personal expense, without any financial support from any institution.

Availability of data and materials

The datasets created and analyzed in the course of this study can be obtained from the corresponding author upon a reasonable request.

References

1. Brennan A, Cross PC, Portacci K, Scurlock BM, and Edwards WH. Shifting brucellosis risk in livestock coincides with spreading seroprevalence in elk. *PLoS One*. 2017;12(6): e 0178780. doi: 10.1371/journal.pone.0178780.
2. Landis M, and Rogovskyy AS. The brief case: Brucella suis infection in a household of dogs. *J Clin Microbiol*. 2022;60(5): e0098421. doi:10.1128/jcm.00984-21
3. Graham LT, Vitale SN, Foss KD, Hague DW, Anderson KM, and Maddox CW. Canine brucellosis in three littermates, case report. *Front Vet Sci*. 2022; 9:958390. doi:10.3389/fvets.2022.958390
4. Ahmed-Bentley J, Roman S, Mirzanejad Y, Fraser E, Hoang L, and Young E, et al. Laboratory exposures from an unsuspected

case of human infection with Brucella canis. *Emerg Infect Dis*. 2021;27(9):2489-2491. doi:10.3201/eid2709.204701
5. Mabe L, Onyiche TE, Thekisoe O, and Suleman E. Accuracy of molecular diagnostic methods for the detection of bovine brucellosis: a systematic review and meta-analysis. *Vet World*. 2022;15(9):2151-2163. doi:10.14202/vetworld.2022.2151-2163
6. de Figueiredo P, Ficht TA, Rice-Ficht A, Rossetti CA, and Adams LG. Pathogenesis and immunobiology of brucellosis: review of Brucella-host interactions. *Am J Pathol*. 2015;185(6):1505-1517. doi: 10.1016/j.ajpath.2015.03.003.
7. Kurmanov B, Zincke D, Su W, Hadfield TL, Aikimbayev A, and Karibayev T, et al. Assays for Identification and Differentiation of Brucella Species: A Review. *Microorganisms*. 2022 Aug 6;10(8):1584. doi: 10.3390/microorganisms10081584.
8. Santos RL, Souza TD, Mol JPS, Eckstein C, and Paíxão TA. Canine brucellosis: an update. *Front Vet Sci*. 2021; 8:594291. doi:10.3389/fvets.2021.594291.
9. Ndazigaruye G., Mushonga B., Kandiwa E., Samkange A., and Segwagwe B. E. Prevalence and risk factors for brucellosis seropositivity in cattle in Nyagatare District, Eastern Province, Rwanda. *Journal of the South African Veterinary Association*. 2018;89(0): e1–e8. doi: 10.4102/ jsava. v89i0.1625.
10. Ogugua AJ, Akinseye VO, Cadmus EO, Jolaoluwa EA, Alabi PI, and Idowu OS et al. Prevalence and risk factors associated with bovine brucellosis in herds under extensive production system in southwestern Nigeria. *Trop Anim Health Prod*. 2018 Oct;50(7):1573-1582. doi: 10.1007/s11250-018-1597-4.
11. Gómez-Miguel MJ, and Moriyón I. Demonstration of a peptidoglycan-linked lipoprotein and characterization of its trypsin fragment in the outer membrane of Brucella spp. *Infect Immun*. 1986 Sep;53(3):678-84. doi: 10.1128/iai.53.3.678-684.1986.
12. Löchel HF, Eger D, Sperlea T, and Heider D. Deep learning on chaos game representation for proteins. Bioinformatics. 2020 Jan 1;36(1):272-279. doi: 10.1093/bioinformatics/btz493.
13. Deschavanne PJ, Giron A, Vilain J, Fagot G, and Fertil B. Genomic signature: characterization and classification of species assessed by chaos game representation of sequences. Mol Biol Evol. 1999 Oct;16(10):1391-9. doi: 10.1093/oxfordjournals.molbev.a026048.
14. Ihalin R, Eneslätt K, and Asikainen S. Peptidoglycan-associated lipoprotein of Aggregatibacter actinomycetemcomitans induces apoptosis and production of proinflammatory cytokines via TLR2 in murine macrophages RAW 264.7 in vitro. *J Oral Microbiol.* 2018 Mar 6;10(1):1442079. doi: 10.1080/20002297.2018.1442079.
15. Pasquevich KA, Garcia SC, Coria LM, Estein SM, Zwerdling A, and Ibanez AE et al. The protein moiety of *Brucella abortus* outer membrane protein 16 is a new bacterial pathogen-associated molecular pattern that activates dendritic cells *in vivo*, induces a Th1 immune response, and is a promising self-adjuvanting vaccine against systemic and oral acquired brucellosis. *J Immunol*, 2010; 184(9):5200– 5212. https:// doi. org/ 10. 4049/ jimmu nol. 09022 09.
16. Hsieh PF, Liu JY, Pan YJ, Wu MC, Lin TL, and Huang YT et al. Klebsiella pneumoniae peptidoglycan-associated lipoprotein and murein lipoprotein contribute to serum resistance, antiphagocytosis, and proinflammatory cytokine stimulation. *J Infect Dis,* 2013; 208(10):1580–1589. https:// doi. org/ 10. 1093/ infdis/jit384.
17. Celli J. Surviving inside a macrophage: the many ways of Brucella. *Res Microbiol*, 2006; 157(2):93–98. https:// doi. org/ 10. 1016/j.resmic. 2005. 10. 002.
18. Luo X, Zhang X, Wu X, Yang X, Han C, and Wang Z et al. Brucella downregulates tumor necrosis factor-α to promote intracellular survival via OMP25 regulation of different microrna s in porcine and murine macrophages. *Front Immunol,* 2017; 8:2013. https:// doi.org/10.3389/ fimmu.2017. 02013.
19. Chen Y, Fu Y, Kong L, Wang F, Peng X, and Zhang Z et al. Pal Affects the Proliferation in Macrophages and Virulence of Brucella, and as Mucosal Adjuvants, Provides an Effective Protection to Mice Against Salmonella Enteritidis. *Curr Microbiol*. 2022 Nov 22;80(1):2. doi: 10.1007/s00284-022-03107-w.
20. Zhi F, Zhou D, Li J, Tian L, Zhang G, and Jin Y et al. Omp16, a conserved peptidoglycan-associated lipoprotein, is involved in Brucella virulence in vitro. *J Microbiol*, 2020; 58(9):793– 804. https:// doi. org/ 10. 1007/ s12275- 020- 0144-y.
21. Zhi F, Fang J, Zheng W, Li J, Zhang G, and Zhou D et al. A Brucella OMP16 conditional deletion strain is attenuated in BALB/c mice. *J Microbiol Biotechnol*, 2022; 32(1):6–14. https://doi.org/ 10. 4014/ jmb. 2107. 07016.
22. Andrianto, A Yun M, Suryawan G, Triastuti F. Rosuvastatin Administration and Its Effect on the IL-6, IL-1β, and TNF-α Cytokines Levels in Peripheral Blood Mononuclear Cells of Type II Diabetes Mellitus Patients with COVID-19. *Moderna Med.* 2024; 23(1): 27-35. https://doi.org/10.31689/rmm.2024.31.1.27.
23. Mharchi S, Maamri A. Diet, Physical Activity, and Their Impact on Chronic Diseases (Hypertension and T2DM) among North-Eastern Morocco's Population. Moderna Med. 2024; 23(1): 37-48. https://doi.org/10.31689/rmm.2024.31.1.37.
24. Spataru T, Stemate A, Sadagurschi R, and Negreanu L. Not Your Typical Ulcerative Colitis Patient. Moderna Med. 2024; 23(1): 79-82. https://doi.org/10.31689/rmm.2024.31.1.79.